CrossMark

Graphitic Carbon Nitride as a New Sensitive Material for Electrochemical Determination of Trace Amounts of Tartrazine in Food Samples

Mohammad Ali Karimi[1] · Vida Haji Aghaei[1] · Azizollah Nezhadali[1] · Narges Ajami[1]

Abstract

In this work, g-C_3N_4 was successfully fabricated by direct pyrolysis of the melamine, and then without any modification, was used to prepare g-C_3N_4/graphite pencil electrode. The maximum current at this working electrode was depended significantly by the pH value; thus, the g-C_3N_4/tartrazine interaction is pH-dependent and the best pH was obtained in an acidic medium at pH 2.1. Cyclic voltammetry and differential pulse voltammetry were used to investigate the electrochemical behavior of tartrazine. Differential pulse voltammetry under the optimized experimental conditions showed that the electrochemical current of the sensor was linear to the concentration of tartrazine in dynamic range of 1.0×10^{-7} to 1.0×10^{-5} mol L^{-1}. The detection limit of tartrazine was found to be 0.21 µmol L^{-1}. In addition, this method is simple, environmental friendly, and economical for rapid and precision determination of trace amounts of tartrazine in real samples. This electrode has a good stability and repeatability.

Keywords Graphitic carbon nitride · Electrochemical determination · Tatrazine · pH-sensitive sensor

Introduction

Graphitic carbon nitride (g-C_3N_4) has been discovered very long ago, in the 1830s (Yew et al. 2016). Binary nitrogen and carbon materials are a new variety of carbonaceous materials doped with nitrogen. Since C and N are the most abundant elements in our planet, these covalent solids are environment friendly (Silva and Rojas, 2016). Graphite-like carbon nitride (g-C_3N_4) is the most stable allotrope of all the carbon nitride under ambient condition (Cheng et al. 2014). The g-C_3N_4 is a new two-dimensional material and has aroused a great deal of interest in recent decades (Liu et al., 2016a; Wang and Bi, 2015). It is environmentally friendly, with excellent biocompatibility and nontoxicity, earth abundant, and can be produced on a large scale at low cost (Cai et al. 2015; Xiong et al. 2016; Li et al. 2015).

The g-C_3N_4 has attracted many interests recently (Amiri et al. 2016). There are strong C–N covalent bonds within each layer of g-C_3N_4, instead of C–C covalent bonds present in graphite. The different layers are held together by weak van der Waals forces (Hatamie et al. 2018).

✉ Mohammad Ali Karimi
ma_karimi43@yahoo.com; m_karimi@pnu.ac.ir

1 Department of Chemistry, Payame Noor University, 19395-4697, Tehran, Iran

Graphitic carbon nitride, an analogue of graphene, has been of great interest due to the strong electron donor nature of nitrogen present in g-C_3N_4, which is absent in graphene (Gu et al. 2015). It is a defect rich, N-bridged poly (tri-s-triazine), whereby the defects and nitrogen atoms serve as active sites for electron conductivity (Lee et al. 2016). In addition, the presence of nitrogen in g-C_3N_4 itself plays an important role in improving the wettability of the electrode with the electrolytes and electron donor and provides more active reaction sites (Ansari and Cho, 2017). The tri-s-triazine ring structure and the high degree of condensation give rise to a medium band gap polymer, an indirect semiconductor (Liu et al., 2016b).

The conjugated aromatic tri-s-triazine polymer-like graphene tends to form p-conjugated planar layers (Wang et al. 2012). Due to its exceptional optical, thermal, electrical, mechanical, and chemical inert properties (Guan et al. 2015), g-C_3N_4 has drawn a huge attraction and is found in many applications, such as lithium-ion battery (Hou et al. 2014), water splitting (Ahmad et al. 2015; Xu et al. 2013; Gao et al. 2017), fuel cells (Mansor et al. 2016), degradation of pollutants (Cao et al. 2015; Zhu et al. 2014), conversion of carbon dioxide to fuels (Ye et al. 2015), NO decomposition (Sano et al. 2013), hydrogenation reactions (Wang et al. 2011), and fluorescent sensor (Rong et al. 2015).

Recently, application of g-C_3N_4 in electrochemical sensors has been reported by a few researchers (Medeiros et al. 2013;

Scheme 1 A general scheme for the reduction of tartrazine on the surface of g-C₃N₄/graphite in acidic medium
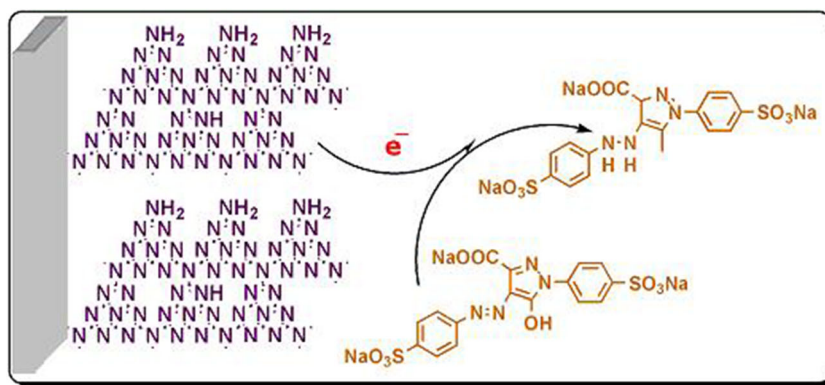
Liu et al. 2014; Zhang et al. 2014; Ma et al. 2015). Recent studies have shown that g-C₃N₄ can be used as an electrochemical sensing platform to study H_2O_2 (Liu et al., 2016a), mercuric ions (Sadhukhan and Barman, 2013), glucose (Tian et al. 2013), ascorbic acid, dopamine, uric acid, and adenine (Lee et al. 2016).

Synthetic colorants have been used to replace natural ones for many years in the food industry, because they show many advantages such as high stability to light, oxygen and pH, color uniformity, low microbiological contamination, and relative lower production costs (Gan et al., 2013a; Chao and Ma, 2015). Tartrazine is a synthetic organic food dye that can be found in common food products, such as beverages, candies, dairy products, and bakery products (Qiu et al. 2016; Taner Bişgin et al. 2015). However, tartrazine really has mutagenic and carcinogenic possibility due to the presence of azo group (–N=N–) (Wang and Zhao, 2015; Al-Degs 2009). So, high concentrations of tartrazine in our life can bring serious problems to human health and some studies show that tartrazine can cause the appearance of allergies, asthma, and childhood hyperactivity (Qiu et al. 2016; Wang and Bi, 2015; Yu et al. 2016).

Until now, different methods, such as high performance liquid chromatography (HPLC) (Al-Degs 2009; Hurst et al. 1981), spectrophotometry (Capitfin-Vallvey et al., 1997), high performance liquid chromatography–mass spectrometry (HPLC–MS) (Qiu et al. 2016), and capillary electrophoresis (Zhao et al. 2014), have been reported for the determination of tartrazine.

In recent years, electrochemical determination methods have also been proposed for the determination of tartrazine for their advantages of high sensitivity, simplicity, low cost, and convenience (Wang and Zhao, 2015; Arvand et al. 2016; Arvand et al. 2017). This method, such as graphene decorated with nickel nanoparticle-modified GCE (Gan et al., 2013a), graphene and mesoporous TiO₂-modified carbon paste electrode (Gan et al., 2013b), graphene oxide and multi-walled carbon nanotube nanocomposite-modified GCE (Qiu et al. 2016), and nanogold-modified CPE (Ghoreishi et al. 2013), has been reported for electrochemical determination of tartrazine azo dye.

Photodegradation of azo dye with g-C₃N₄ was seen in many articles (Jiang et al. 2017; Tao et al. 2015; Yan et al. 2010), but until now, g-C₃N₄ without modification has not
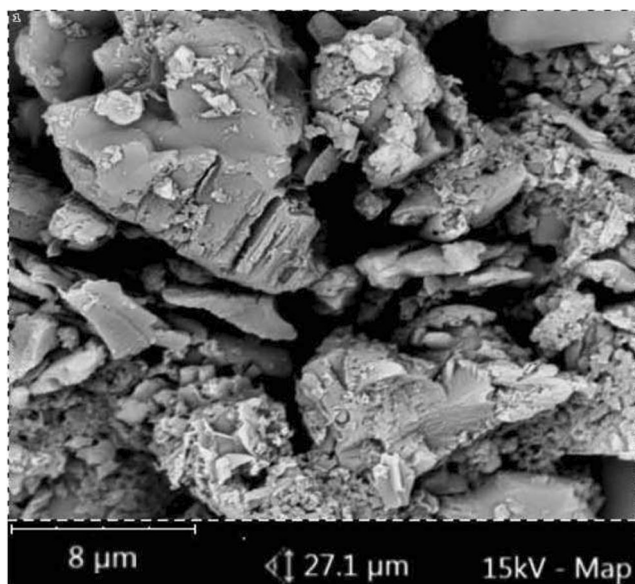
Fig. 1 XRD pattern of g-C₃N₄
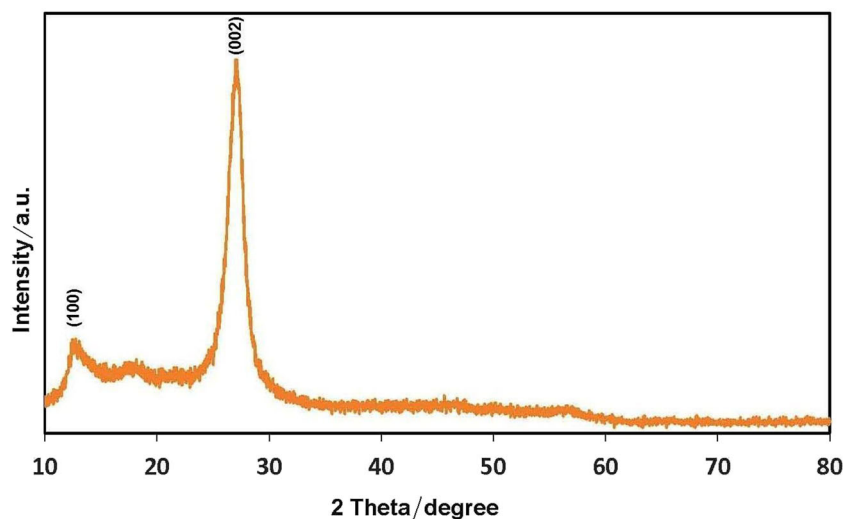
Fig. 2 SEM image of g-C$_3$N$_4$

been used to identify this color by electrochemical method. In this work, for the first time, we applied g-C$_3$N$_4$ as a modifier for graphite pencil electrode (in this paper, graphite pencil is called graphite). Also, this electrode due to the existence of strong electron donor nitrogen group in g-C$_3$N$_4$ framework can increased the rate of the electron transfer for reduction reaction of tartrazine (Zhao et al. 2017) (Scheme 1). Therefore, this new electrode was used for electrochemical determination of tartrazine synthetic food dye in real samples.

Experimental

Materials

Melamine (Lobachemie Reagents company, India), tartrazine (Sigma-Aldrich), potassium chloride, potassium dihydrogen phosphate, and phosphoric acid (Merck) were purchased. All chemicals were of analytical grade and used without further purification. Phosphate buffer with pH 2.1 (0.1 mol L^{-1}) was prepared using potassium dihydrogen phosphate and phosphoric acid. Tartrazine was dissolved into deionized water to prepare standard solutions and stored at 4 °C. Deionized water was used for the preparation of all solutions.

Apparatus

Electrochemical measurements were performed on a PGSTAT302 (Metrohm-Netherlands) electrochemical workstation. A platinum electrode, an Ag/AgCl electrode, and modified graphite electrode served as the auxiliary electrode, reference electrode, and working electrode, respectively. X-ray diffraction (XRD) patterns of the powder were collected with a scanning speed of 2°/min and a step of 0.02° (2θ) in the range from 10 to 80° on a Shimadzu (XRD-6000), X-ray diffractometer with Cu/Kα radiation (1.54 Å). The structural morphology of the g-C$_3$N$_4$ was investigated by using scanning electron microscopy (SEM) with Phenom ProX with a high performance. The Fourier transform infrared (FT-IR) spectroscopy was recorded using a Shimadzu IR Prestige-21 apparatus with the prepared powder diluted in KBr pellets.

Procedures

Synthesis of g-C$_3$N$_4$?

The metal-free g-C$_3$N$_4$ powder was synthesized via direct pyrolysis of the melamine based on the report (Amiri et al. 2016). Typically, 5 g of melamine was put into an alumina crucible with a cover then heated in a muffle furnace for 4 h at 550 °C. After cooling down to room temperature, the pale yellow g-C$_3$N$_4$ were collected and milled into powder for further use. The g-C$_3$N$_4$ phase, morphology, composition, and structure were characterized by using SEM, XRD, and FT-IR spectroscopy.
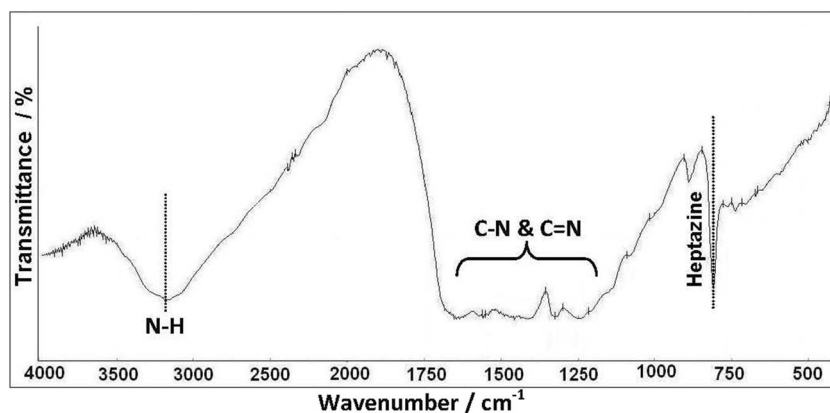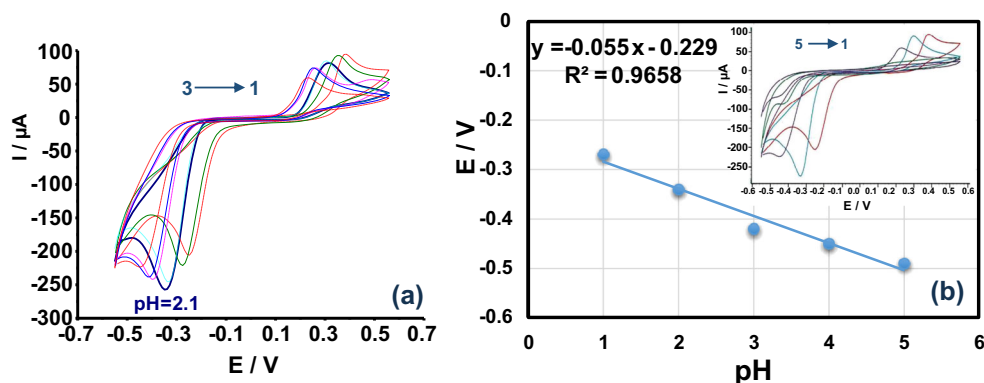
Fig. 3 FT-IR spectrum of g-C$_3$N$_4$

Fig. 4 a Cyclic voltammogram of 0.5 mmol L^{-1} tartrazine in 0.1 mol L^{-1} phosphate buffer on the surface of g-C$_3$N$_4$/graphite in various pH in the range of 1.0–3.0. b Plot of the peak potential vs. pH

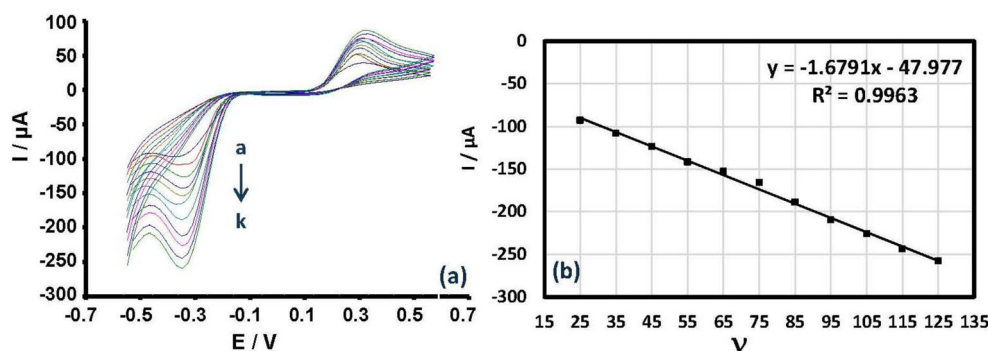## Preparation of g-C$_3$N$_4$?/Graphite Electrode

Firstly, the graphite electrode has been polished on a paper to obtain a shiny and smooth surface, and then rinsed with de-ionized water and acetone after polishing step. Then, the graphite electrode was dried at room temperature. Secondly, suspension (1 mg mL^{-1}) of g-C$_3$N$_4$ was prepared from the dispersion of g-C$_3$N$_4$ powder in ethanol/water mixture (1:1), and sonication for 45 min. Finally, 5.0 μL of a 1 mg mL^{-1} of g-C$_3$N$_4$ suspension, as a modifier material, was deposited on to the graphite surface electrode and then allowed to dry at room temperature. The deposition step was repeated for ten times (50.0 μL) and uniform film of g-C$_3$N$_4$ material was formed on the surface of graphite electrode for electrochemical measurement.

Results and Discussion

Characterization of g-C$_3$N$_4$? Structure

Phase structure of the g-C$_3$N$_4$ was studied by XRD pattern, and the result along with its standard pattern is displayed in Fig. 1. Typically, g-C$_3$N$_4$ powder shows two diffraction peaks at about 27.3° corresponding to the stacking of the conjugated aromatic system, and a peak at about 13.1° corresponding to the interlayer structural packing (Amiri et al. 2016; Wang et al. 2009).

The morphologies of as-synthesized g-C$_3$N$_4$ were characterized by SEM. The SEM images of the morphology and the microstructure of the as-prepared sample (Fig. 2) indicate the layered, stacked texture, and the smooth surface morphology of bulk g-C$_3$N$_4$ (Hong et al. 2015).

In the FT-IR spectrum of pure g-C$_3$N$_4$ (Fig. 3), the broad band at 1200–1650 cm^{-1} is attributed to the stretching vibration modes of C−N and C=N in heterocycles (Vadivel et al. 2016). Furthermore, the band at 806 cm^{-1} is related to the breathing mode of the heptazine arrangement. The broad band at 3000–3300 cm^{-1} is due to the terminal NH$_2$ or NH groups at the defect sites of g-C$_3$N$_4$ aromatic rings (Amiri et al. 2016).

Effect of pH

The electrochemical responses of 0.5 mmol L^{-1} tartrazine at g-C$_3$N$_4$/graphite electrode in different supporting electrolytes, with the same concentration (0.1 mol L^{-1}), such as phosphoric acid and potassium di-hydrogen phosphate buffer solution, acetic acid and sodium acetate buffer solution, and hydrochloric acid solution, were examined by CV. The results show that phosphate buffer gives greater sensitivity to tartrazine. The solution of tartrazine was prepared in the referred supporting electrolyte and analyzed. Then, the influence of solution acidity on the reduction behaviors of 0.5 mmol L^{-1} tartrazine in 0.1 mol L^{-1} phosphate buffer in the range of pH 1–3 was tested. The results indicated that the reduction Ip of tartrazine

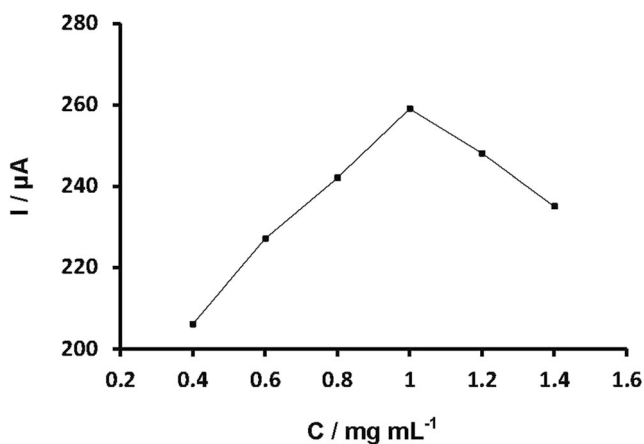Fig. 5 a Cyclic voltammogram of 0.5 mmol L^{-1} tartrazine in 0.1 mol L^{-1} phosphate buffer pH 2.1 on the surface of g-C$_3$N$_4$ /graphite with various scan rates of 25, 35, 45, 55, 65, 75, 85, 95, 105, 115, and 125 mV s^{-1} (a → k). b Plot of Ip vs. scan rate

Fig. 6 Effect of different amounts of g-C_3N_4 in the range of 0.4–1.4 mg mL^{-1} on the cyclic voltammogram of 0.5 mmol L^{-1} tartrazine in 0.1 mol L^{-1} phosphate buffer pH 2.1 with 125 mV s^{-1} scan rate

Fig. 8 Chemical structure of tartrazine

increased with the pH increasing from 1.0 to 2.1, and then decreased when the pH was further increased up to 3 (Fig. 4a). So, the 0.1 mol L^{-1} phosphate buffer with a pH of 2.1 was chosen as the supporting electrolyte.

As shown in Fig. 4b, by increasing pH, the reduction peak of tartrazine shifted toward a less positive potential, indicating that protons are involved in the reduction of tartrazine. The reduction Ep of tartrazine showed linear relationship with the solution pH. The regression equation for this relationship is obtained as:

$$E, V = -0.055pH - 0.229, \quad R^2 = 0.9658$$

The slope of peak potential curves versus pH for tartrazine was 55 mV/pH which indicates that equal numbers of electrons and protons are involved in the electro-reduction of tartrazine on the surface of the modified electrode.
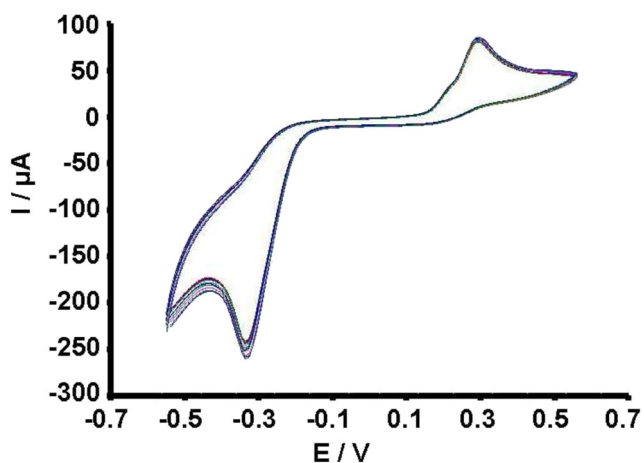
Effect of Scan Rate

In Fig. 5a, the cyclic voltammogram of 0.5 mmol L^{-1} tartrazine has been showed in buffer solution with pH 2.1 on the surface of the g-C_3N_4/graphite electrode with various scan rates. In this figure, the maximum signal of reduction Ip was observed in 125 mV s^{-1}, because at this voltage scan rates, the charge passed per unit time is greater and thus an increase in Ip is seen. The relation between peak currents and scan rates is approximately linear and the adsorption-controlled mechanism can be suggested for tartrazine reduction.

Effect of Amount of g-C_3N_4?

The reduction current of tartrazine at modified electrode can be affected by the amount of g-C_3N_4 on the electrode surface. This can be controlled by using the same volume (50.0 μL) of g-C_3N_4 suspensions with the different concentrations in the range of 0.4–1.4 mg mL^{-1} on the surface of graphite. Electrochemical behavior of 0.5 mmol L^{-1} tartrazine in 0.1 mol L^{-1} phosphate buffer with different concentrations of

Fig. 7 Cyclic voltammogram of 0.5 mmol L^{-1} tartrazine in 0.1 mol L^{-1} phosphate buffer pH 2.1 on the surface of g-C_3N_4/graphite with 125 mV s^{-1} scan rate
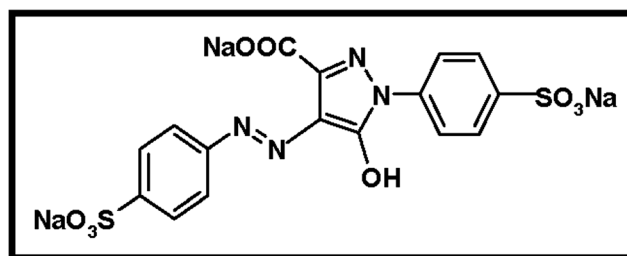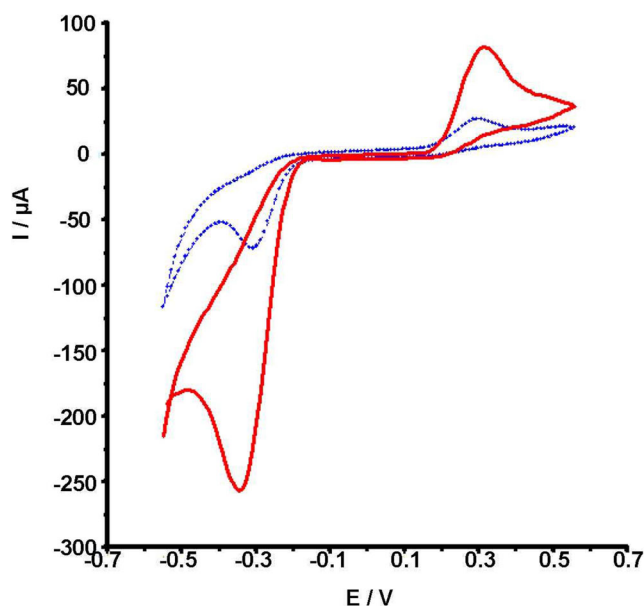

Fig. 9 Cyclic voltammogram of 0.5 mmol L^{-1} tartrazine in 0.1 mol L^{-1} phosphate buffer pH 2.1 with 125 mV s^{-1} scan rate on the surface of **a** graphite (dashed line) and **b** g-C_3N_4/graphite (solid line)

Fig. 10 **a** DPV of tartrazine in 0.1 mol L^{-1} phosphate buffer pH 2.1 on the surface of g-C$_3$N$_4$/graphite in concentrations of 1.0×10^{-7}, 3.0×10^{-7}, 5.0×10^{-7}, 8.0×10^{-7}, 1.0×10^{-6}, 3.0×10^{-6}, 5.0×10^{-6}, 8.0×10^{-6}, and 1.0×10^{-5} mol L^{-1}. **b** Calibration plot of Ip vs. tartrazine concentration. DPV setting pulse amplitude, 100 mV; step potential, 15 mV; and modulation time, 50 ms.
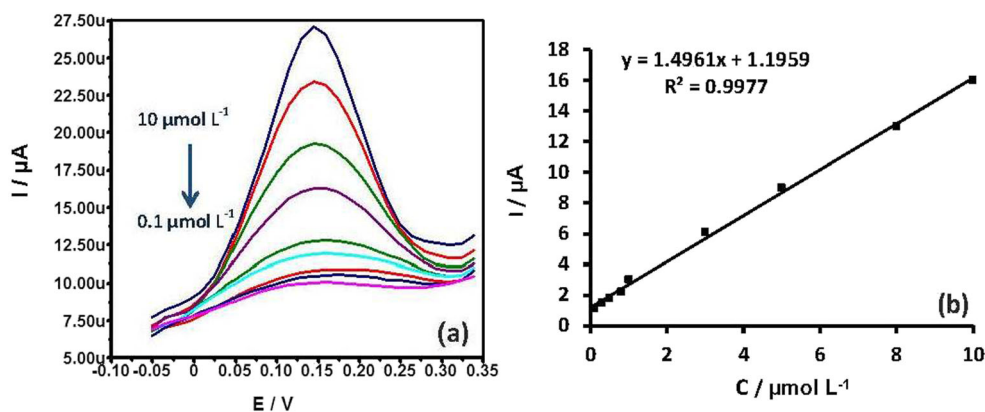
g-C$_3$N$_4$ in the range of 0.4, 0.6, 0.8, 1, 1.2, and 1.4 mg mL^{-1} were investigated by cyclic voltammetry. The results indicated that the reduction Ip of tartrazine enhanced with increase in the concentration of g-C$_3$N$_4$ up to 1.0 mg mL^{-1}. Further increase, caused a decrease in the electrochemical response of electrode (Fig. 6). This behavior is related to the thickness of the film. If the film is thin, the amount of tartrazine adsorbed is small, and as a result, a small Ip is observed. When the film is thick, its conductivity gets reduced, and also, the g-C$_3$N$_4$ becomes unstable and could leave off the electrode surface. Therefore, 50.0 μL of 1.0 mg mL^{-1} of g-C$_3$N$_4$ suspension was selected as optimum amount for preparation of the modified electrode.

Reproducibility and Stability of Graphite and g-C$_3$N$_4$?/Graphite Electrode

The reproducibility and stability of graphite and g-C$_3$N$_4$/graphite were carried out in the solution of 0.5 mmol L^{-1} concentration level of tartrazine in buffer solution with pH 2.1 for 40 cycles. The relative standard deviation (RSD) of

graphite and g-C$_3$N$_4$/graphite electrode after ten repetitions was 3.6 and 2.5%, respectively. These results show that g-C$_3$N$_4$/graphite electrode has a good stability and reproducibility for the determination of tartrazine (Fig. 7). The stability of g-C$_3$N$_4$/graphite electrode of its initial response from 2 months ago was investigated and RSD of electrode was measured 4.1%. The excellent long-term stability of g-C$_3$N$_4$ on the electrode surface and reproducibility of the g-C$_3$N$_4$/graphite make it attractive in the field of analytical applications.

Cyclic Voltammetric Behaviors of Tartrazine at the Surface of Graphite and g-C$_3$N$_4$?/Graphite

Regarding the chemical structure that is shown in Fig. 8, we clearly found that tartrazine contains azo group which is electrochemical active and can be reduced on g-C$_3$N$_4$/graphite electrode surface. Figure 9 indicates the electrochemical behavior of 0.5 mmol L^{-1} tartrazine on the surface of graphite (dashed line) and g-C$_3$N$_4$/graphite (solid line) electrodes by using cyclic voltammetry in 0.1 mol L^{-1} phosphate buffer

Table 1 Comparison of different electrodes in tartrazine detection

Electrode	Sensitivity (μA/μmol L^{-1})	Detection limit (μmol L^{-1})	Linear range (μmol L^{-1})	Ref.
Boron-doped diamond	0.108	2.5	5.0–60.0	Medeiros et al., 2012
Polyallylamine-modified tubular	—	1.8	10.0–200.0	Lu'ısa et al., 2007
MWCNTs-IL/CCE	0.216	1.1	0.4–70.0	Majidi et al., 2013
MWCNT/pyrolytic graphite	3.258	0.93	3.7–430.0	Songa et al., 2012
Antimony film (SbFE)	—	0.3	1.0–5.0	Rodrguez et al., 2015
MWCNT/GCE	3.5	0.22	1.0–7.0	Sierra-Rosalesa et al., 2017
g-C$_3$N$_4$/graphite	1.49	0.21	0.1–10.0	This work

with pH 2.1. On the surface of graphite, tartrazine exhibits a reduction Ep at approximately − 0.31 V and Ip − 71.8 μA. On the other hand, the reduction peak at a lower negative potential near − 0.34 V with Ip – 260 μA on the surface of g-C$_3$N$_4$/graphite is recorded and Ep at the g-C$_3$N$_4$/graphite shifted by about 30 mV toward negative values when compared with the unmodified graphite electrode. In comparison, at the g-C$_3$N$_4$/graphite, the voltammetric response of tartrazine was greatly improved. It can be correlated to decrease of overpotential at the surface of g-C$_3$N$_4$/graphite electrode. Also, this electrode, due to the existence of strong electron donor nitrogen group in g-C$_3$N$_4$ framework, can increased the rate of the electron transfer for reduction reaction of tartrazine and provide more electrochemical active site to improve the electrochemical activity of g-C$_3$N$_4$ (Zhao et al. 2017). Therefore, in this work, g-C$_3$N$_4$/graphite electrode was chosen for all electrochemical measurements, so that the tartrazine was measured in different concentrations on the surface of this electrode.

Calibration Curve and Detection Limit for Determination of Tartrazine

Under the optimized experimental conditions, differential pulse voltammetric (DPV) was used for quantitative determination of the tartrazine. In Fig. 10, a linear relationship is seen between reduction Ip and concentration of tartrazine in dynamic ranges of 1.0×10^{-7}–1.0×10^{-5} mol L^{-1}. The linear equation can be expressed as I$_{pc}$ (μA) = 1.4961 C (μM) + 1.1959; (R^2 = 0.9977).

Figure 10 shows that the electrochemical Ip of tartrazine increased remarkably with the increase of tartrazine concentrations. The detection limit (LOD) was calculated as three times the standard deviations of the blank solution divided by the slope of the calibration curve (Sierra-Rosalesa et al. 2017). For tartrazine, the detection limit was found to be 0.21 μmol L^{-1}. The result was compared with the reported electrodes which were shown in Table 1. It can be seen that this new sensing system exhibited lower detection limit for tartrazine than the electrodes reported in Table 1.

The presented modifier exhibits the good analytical results, easy fabrication method, easy to use, and also, the preparation time and drying process is considerably short compare to the other electrodes. On the other hand, graphite electrode has many advantages such as low cost, user friendly, and ease in handling and disposability. The total of these properties has led to use of this electrode in the determination of tartrazine dye.

Real Sample Analysis

The electrochemical method is one of the identifying methods for determination of fraud in saffron. The proposed method in
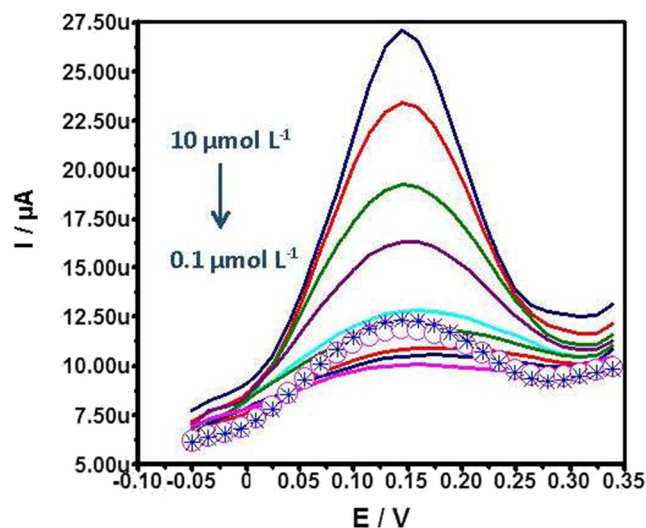

Fig. 11 Curves of two samples of saffron fake powder in the tartrazine plot **a** sample 1 (circle) and **b** sample 2 (star)

this paper was used to identify two samples of saffron fake powder without the standard logo of Iran that was purchased from a salesman in the city. For determination of saffron fake powder, 0.7 mg of it was introduced into a 25-mL volumetric flask and filled up with phosphate buffer 0.1 mol L^{-1} (pH 2.1) to desired volume and this process was repeated for another sample. Under the optimized conditions, the prepared test solution of saffron fake powder was detected on the surface of g-C$_3$N$_4$/graphite electrode by DPV. For each samples, during the potential sweep from − 0.1 to 0.35 V, the DPV curves were recorded and the good peak of tartrazine was observed. This indicates that the modified electrode can be used for practical application. The content of tartrazine was obtained by the standard addition method and recoveries of two samples were found 98.2 and 102.3% with the presented method for first and second saffron fake powder samples, respectively. This satisfactory recovery demonstrated that this method is very promising for detection of tartrazine in real samples, and as seen in Fig. 11, two saffron fake powder samples are content tartrazine dye.

Conclusions

The g-C$_3$N$_4$/graphite-sensitive sensor was conveniently created by facile processing route. The outstanding character of the proposed synthesis method lies in the green route and short reaction time. The maximum current at this working electrode depended significantly by the pH value, and therefore, we conclude that the g-C$_3$N$_4$/Tartrazine interaction is pH-dependent. It shows a good electrochemical activity toward the reduction of Tartrazine in an acidic medium at pH 2.1. In addition, this method is simple, environmental friendly, and economical for rapid and precision determination of trace

amounts of Tartrazine in real samples. Also, the strong electron donor nature of nitrogen present in semiconductor-g-C$_3$N$_4$ framework provides more electrochemical active sites to improve the electrochemical activity of g-C$_3$N$_4$ and increased electron-transfer rate and therefore electrochemical response to dye was enhanced.

Compliance with Ethical Standards

Conflict of Interest M.A. Karimi declares that he has no conflict of interest. V. Haji Aghaei declares that he she has no conflict of interest. A. Nezhadali declares that he has no conflict of interest. N. Ajami declares that she has no conflict of interest.

Ethical Approval All procedures performed in studies were in accordance with the ethical standards of the institutional and/or national research committee and with the 1964 Helsinki Declaration and its later amendments or comparable ethical standards. This article does not contain any studies with human or animal subjects performed by any of the authors.

Informed Consent Not applicable.

References

Ahmad HS, Kamarudin K, Minggu LJ, Kassim M (2015) Hydrogen from photo-catalytic water splitting process: a review. Renew Sustain Energy Rev 43:599–610

Al-Degs YS (2009) Determination of three dyes in commercial soft drinks using HLA/GO and liquid chromatography. Food Chem 117:485–490

Amiri M, Salehniya H, Habibi-Yangjeh A (2016) Graphitic carbon nitride/chitosan composite for adsorption and electrochemical determination of mercury in real samples. Ind Eng Chem Res 55:8114–8122

Ansari SA, Cho MH (2017) Simple and large scale construction of MoS$_2$-g-C$_3$?N$_4$? heterostructures using mechanochemistry for high performance electrochemical supercapacitor and visible light photocatalytic applications. Sci Rep 7:43055

Arvand M, Parhizi Y, Mirfathi SH (2016) Simultaneous voltammetric determination of synthetic colorants in foods using a magnetic core–shell Fe$_3$O$_4$?@SiO$_2$?/MWCNTs nanocomposite modified carbon paste electrode. Food Anal Methods 9:863–875

Arvand M, Ashoori Gaskarmahalleh A, Hemmati S (2017) Enhanced-oxidation and highly sensitive detection of Tartrazine in foodstuffs via new platform based on poly (5-sulfosalicylic acid) /Cu(OH)$_2$? nanoparticles. Food Anal Methods 10:2241–2251

Cai Z, Rong M, Zhao T, Zhao L, Wang Y, Chen X (2015) Solar-induced photoelectrochemical sensing for dopamine based on TiO$_2$ nanoparticles on g-C$_3$N$_4$? decorated graphene nanosheets. J Electroanal Chem 759:32–37

Cao S, Low J, Yu J, Jaroniec M (2015) Polymeric photocatalysts based on graphitic carbon nitride. Adv Mater 27:2150–2176

Capitfin-Vallvey LF, Iglesias NN, Paya IO, Castaneda RA (1997) Simultaneous determination of Tartrazine and sunset yellow in cosmetic products by first-derivative spectrophotometry. Microchim Acta 126:153–157

Chao M, Ma X (2015) Convenient electrochemical determination of sunset yellow and Tartrazine in food samples using a poly (L-phenylalanine)-modified glassy carbon electrode. Food Anal Methods 8:130–138

Cheng N, Jiang P, Liu Q, Tian J, Asiri AM, Sun X (2014) Graphitic carbon nitride nanosheets: one-step, high-yield synthesis and application for Cu^{2+} detection. Analyst 139:5065–5068

Gan T, Sun J, Meng W, Song L, Zhang Y (2013a) Electrochemical sensor based on graphene and mesoporous TiO$_2$ for the simultaneous determination of trace colourants in food. Food Chem 141:3731–3737

Gan T, Sun J, Wu Q, Jing Q, Yu S (2013b) Graphene decorated with nickel nanoparticles as a sensitive substrate for simultaneous determination of sunset yellow and tartrazine in food samples. Electroanalysis 25:1505–1512

Gao X, Liu X, Zhu Z, Gao Y, Wang Q, Zhu F, Xie Z (2017) Enhanced visible light photocatalytic performance of CdS sensitized TiO$_2$ nanorod arrays decorated with Au nanoparticles as electron sinks. Sci Rep 7:973

Ghoreishi SM, Behpour M, Golestaneh M (2013) Selective voltammetric determination of tartrazine in the presence of red 10B by nanogold-modified carbon paste electrode. J Chin Chem Soc 60:120–126

Gu H, Zhou T, Shi G (2015) Synthesis of graphene supported ?graphene-likeC$_3$?N$_4$? metal-free layered nanosheets for enhanced electrochemical performance and their biosensing for biomolecules. Talanta 132:871–876

Guan W, Long Z, Liu J, Hua Y, Ma Y, Zhang H (2015) Unique graphitic carbon nitride nanovessels as recyclable adsorbent for solid phase extraction of benzoylurea pesticides in juices samples. Food Anal Methods 8:2202–2210

Hatamie A, Marahel F, Sharifat A (2018) Green synthesis of graphitic carbon nitride nanosheet (g-C$_3$?N$_4$)? and using it as a label-free fluorosensor for detection of metronidazole via quenching of the fluorescence. Talanta 176:518–525

Hong Y, Jiang Y, Li C, Fan W, Yan X, Yan M, Shi W (2015) In-situ synthesis of direct solid-state Z-scheme, V$_2$O$_5$?/g-C$_3$?N$_4$? heterojunctions with enhanced visible light efficiency in photocatalytic degradation of pollutants. Appl Catal B-Environ 180:663–673

Hou Y, Li J, Wen Z, Cui S, Yuan C, Chen J (2014) N-doped graphene/porous g-C$_3$N$_4$? nanosheets supported layered-MoS$_2$ hybrid as robust anode materials for lithium-ion batteries. Nano Energy 8:157–164

Hurst WJ, Mckim JM, Martin RA (1981) Determination of tartrazine in food products by HPLC. J Food Sci 46:419–424

Jiang X, Li J, Fang J, Gao L, Cai W, Li X, Xu A, Ruan X (2017) The photocatalytic performance of g-C$_3$N$_4$? from melamine hydrochloride for dyes degradation with peroxymonosulfate. J Photochem Photobiol A Chem 336:54–62

Lee HL, Sofer Z, Mazanek V, Luxa J, Chua CK, Pumera M (2016) Graphitic carbon nitride: effects of various precursors on the structural, morphological and electrochemical sensing properties. Appl Mater Today 8:150–162

Li Q, He Y, Peng R (2015) TeO$_2$ nanoparticle loaded graphitic carbon nitride hybrids: their preparation and catalytic activities in the thermal decomposition of ammonium perchlorate. Eur J Inorg Chem 34:4062–4067

Liu Y, Wang Q, Lei J, Hao Q, Wang W, Ju H (2014) Anodic electrochemiluminescence of graphitic-phase C$_3$N$_4$? Nanosheets for sensitive biosensing. Talanta 122:130–134

Liu L, LV H, Wang C, AO Z, Wang G (2016a) Fabrication of the protonated graphitic carbon nitride nanosheets as enhanced electrochemical sensing platforms for hydrogen peroxide and paracetamol detection. Electrochim Acta 206:259–269

Liu J, Wang H, Antonietti M (2016b) Graphitic carbon nitride "reloaded": emerging applications beyond (photo) catalysis. Chem Soc Rev 45:2308–2326

Lu'ısa M, Silva S, Beatriz M, Garcia Q, LFC L, Lima E (2007) Voltammetric determination of food colorants using a polyallylamine modified tubular electrode in a multicommutated flow system. Talanta 72:282–288

Ma H, Wang Y, Zhang H, Wu D, Guo A, Yan T, Wei Q, Du B (2015) A sensitive electrochemical immunesensor for the detection of squamous cell carcinoma antigen by using PtAu nanoparticles loaded on ?TiO₂? colloidal spheres as labels. RSC Adv 5:59853–59860

Majidi MR, Fadakar Bajeh Baj R, Naseri A (2013) Carbon nanotube–ionic liquid (CNT–IL) nanocamposite modified sol-gel derived carbon-ceramic electrode for simultaneous determination of sunset yellow and tartrazine in food samples. Food Anal Methods 6:1388–1397

Mansor N, Miller TS, Dedigama I, BelenJorge A, Jia J, Brázdová V, Mattevi C, Gibbs C, Hodgson D, Shearing PR, Howardg A, Coràb F, Daniel MS, Bretta JL, McMill F (2016) Graphitic carbon nitride as a catalyst support in fuel cells and electrolyzers. Electrochim Acta 222:44–57

Medeiros RA, Lourenceao BC, Rocha-Filho RC, Fatibello-Filho O (2012) Flow injection simultaneous determination of synthetic colorants in food using multiple pulse amperometric detection with a boron-doped diamond electrode. Talanta 99:883–889

Medeiros RA, Matos R, Benchikh A, Saidani B, Debiemme-Chouvy C, Deslouis C, Rocha-Filho RC (2013) Amorphous carbon nitride as an alternative electrode material in electroanalysis: simultaneous determination of dopamine and ascorbic acid. Anal Chim Acta 797:30–39

Qiu X, Lu L, Leng J, Yu Y, Wang W, Jiang M, Bai L (2016) An enhanced electrochemical platform based on graphene oxide and multi-walled carbon nanotubes nanocomposite for sensitive determination of sunset yellow and tartrazine. Food Chem 190:889–895

Rodrguez JA, Jurez MG, Galn-Vidal CA, Miranda JM, Barrado E (2015) Determination of allura red and tartrazine in food samples by sequential injection analysis combined with voltammetric detection at antimony film electrode. Electroanalysis 27:2329–2334

Rong M, Lin L, Song X, Wang Y, Zhong Y, Yan J, Feng Y, Zeng X, Chen X (2015) Fluorescence sensing of chromium (VI) and ascorbic acid using graphitic carbon nitride nanosheets as a fluorescent "switch". Biosens Bioelectron 68:210–217

Sadhukhan M, Barman S (2013) Bottom-up fabrication of two-dimensional carbon nitride and highly sensitive electrochemical sensors for mercuric ions. J Mater Chem A 1:2752–2756

Sano T, Tsutsui S, Koike K, Hirakawa T, Teramoto Y, Negishi N, Takeuchi K (2013) Activation of graphitic carbon nitride (g-C₃?N₄?) by alkaline hydrothermal treatment for photocatalytic NO oxidation in gas phase. J Mater Chem A 1:6489–6496

Sierra-Rosalesa P, Toledo-Neirab C, Squellaa JA (2017) Electrochemical determination of food colorants in soft drinks using MWCNT-modified GCEs. Sens Actuat B Chem 240:1257–1264

Silva AM, Rojas MI (2016) Electric and structural properties of polymeric graphite carbon nitride (g-C₃?N₄?): a density functional theory study. Comput Theor Chem 1098:41–49

Songa YZ, Xua JM, Lva JS, Zhonga H, Yeb Y, Xiec JM (2012) Electrochemical reduction of tartrazine at multi-walled carbon nanotube-modified pyrolytic graphite electrode. Russ J Phys Chem A 86:303–310

Taner Bişgin A, Uçan M, Narin I, Soylak M (2015) A comparative study for separation, preconcentration and determination of tartrazine (E 102) in soft drink samples by two kinds of amberlite resins. Food Anal Methods 8:2141–2149

Tao Y, Ni Q, Wei M, Xia D, Li X, Xu A (2015) Metal-free activation of peroxymonosulfate by g- C₃?N₄? under visible light irradiation for the degradation of organic dyes. RSC Adv 5:44128–44136

Tian J, Liu Q, Ge C, Xing Z, Asiri AM, Al-Youbi AO, Sun X (2013) Ultrathin graphitic carbon nitride nanosheets: a low-cost, green, and highly efficient electrocatalyst toward the reduction of hydrogen peroxide and its glucose biosensing application. Nano 5:8921–8924

Vadivel S, Maruthamani D, Habibi-Yangjeh A, Paul B, Sankar Dhar S, Selvam K (2016) Facile synthesis of novel CaFe₂O₄?/g-C₃?N₄? nanocomposites for degradation of methylene blue under visible-light irradiation. J Colloid Interface Sci 480:126–136

Wang M, Bi W (2015) Synthesis of g-C₃N₄?/Fe₃?O₄? nanocomposites and application as a new sorbent for solid phase extraction of polycyclic aromatic hydrocarbons in water samples. Talanta 132:922–928

Wang M, Zhao J (2015) Facile synthesis of Au supported on ionic liquid functionalized reduced graphene oxide for simultaneous determination of sunset yellow and tartrazine in drinks. Sens Actuat B Chem 216:578–585

Wang X, Maeda K, Thomas A, Takanabe K, Xin G, Carlsson JM, Domen K, Antonietti M (2009) A metal-free polymeric photocatalyst for hydrogen production from water under visible light. Nat Mater 8:76–80

Wang Y, Yao J, Li H, Su D, Antonietti M (2011) Highly selective hydrogenation of phenol and derivatives over a Pd@carbon nitride catalyst in aqueous media. J Am Chem Soc 133:2362–2365

Wang Y, Wang X, Antonietti M (2012) Polymeric graphitic carbon nitride as a heterogeneous organocatalyst: from photochemistry to multipurpose catalysis to sustainable chemistry. Angew Chem Int Ed 51:68–89

Xiong T, Cen W, Zhang Y, Dong F (2016) Bridging the g-C₃N₄? interlayers for enhanced photocatalysis. ACS Catal 6:2462–2472

Xu J, Li Y, Peng S, Lu G, Li S (2013) Eosin Y-sensitized graphitic carbon nitride fabricated by heating urea for visible light photocatalytic hydrogen evolution: the effect of the pyrolysis temperature of urea. Phys Chem Chem Phys 15:7657–7665

Yan SC, Li ZS, Zou ZG (2010) Photodegradation of rhodamine B and methyl orange over boron-doped g-C₃N₄? under visible light irradiation. Langmuir 26:3894–3901

Ye S, Wang R, Wu M, Yuan Y (2015) A review on g-C₃N₄? for photocatalytic water splitting and CO₂ reduction. Appl Surf Sci 358:15–27

Yew YT, Lim CS, Eng AYS, Oh J, Park S, Pumera M (2016) Electrochemistry of layered graphitic carbon nitride synthesised from various precursors: searching for catalytic effects. ChemPhysChem 17:481–488

Yu L, Zheng H, Shi M, Jing S, Qu L (2016) A novel electrochemical sensor based on poly (diallyldimethylammoniumchloride)-dispersed graphene supported palladium nanoparticles for simultaneous determination of sunset yellow and tartrazine in soft drinks. Food Anal Methods 10:200–209

Zhang H, Huang Q, Huang Y, Li F, Zhang W, Wei C, Chen J, Dai P, Huang L, Huang Z, Kang L, Hu S, Hao A (2014) Graphitic carbon nitride nanosheets doped graphene oxide for electrochemical simultaneous determination of ascorbic acid, dopamine and uric acid. Electrochim Acta 142:125–131

Zhao L, Zeng B, Zhao F (2014) Electrochemical determination of tartrazine using a molecularly imprinted polymer–multiwalled carbon nanotubes-ionic liquid supported Pt nanoparticles composite film coated electrode. Electrochim Acta 146:611–617

Zhao Q, Wu W, Wei X, Jiang S, Zhou T, Li Q, Lu Q (2017) Graphitic carbon nitride as electrode sensing material for tetrabromobisphenol-A determination. Sens Actuat B Chem 248:673–681

Zhu J, Xiao P, Li H, Carabineiro SAC (2014) Graphitic carbon nitride: synthesis, properties and applications in catalysis. ACS Appl Mater Interfaces 6:16449–16465